Formation of recent martian gullies through melting of extensive water-rich snow deposits

Philip R. Christensen

Department of Geological Sciences, Campus Box 876305, Arizona State University, Tempe, Arizona 85287-6305, USA

The observation of gullies on Mars indicates the presence of liquid water near the surface in recent times[1,2], which is difficult to reconcile with the current cold climate. Gullies have been proposed to form through surface runoff from subsurface aquifers[1,3] or through melting of near-surface ice under warmer conditions[4]. But these gullies are observed to occur preferentially in cold mid-latitudes[2], where the presence of liquid water is less likely, and on isolated surfaces where groundwater seepage would not be expected, making both potential explanations unsatisfactory. Here I show that gullies can form by the melting of water-rich snow that has been transported from the poles to mid-latitudes during periods of high obliquity within the past 10^5 to 10^6 years (refs 5, 6). Melting within this snow[7] can generate sufficient water to erode gullies in about 5,000 years. My proposed model for gully formation is consistent with the age and location of the gullies, and it explains the occurrence of liquid water in the cold mid-latitudes as well as on isolated surfaces. Remnants of the snowpacks are still present on mid-latitude, pole-facing slopes, and the recent or current occurrence of liquid water within them provides a potential abode for life.

Small young gullies commonly occur in clusters on slopes between 30° and 70° latitude in both hemispheres of Mars[2]. They consist of alcoves several hundred metres wide, and channels up to several kilometres long and several tens of metres deep[1,2]. Gullies typically originate within several hundred metres of the slope crest, and can occur on crater walls that are raised above the surrounding terrain or near the summit of isolated knobs. Gullies most probably result from flow of liquid water[1,2], although alternative fluids—such as concentrated brines[8,9], or gaseous or liquid CO_2 (ref. 10)—have been considered.

It has recently been suggested[4] that periods of high obliquity produce sufficient warming on pole-facing slopes to melt near-surface ice deposits and erode gullies by water-rich debris flows. However, this model does not fully address the fact that as the surface and subsurface temperatures increase, the upper soil layer will become desiccated before significant liquid water can be produced.

Here I propose an alternative model in which melting of an overlying snowpack provides the source of water to erode gullies. The main features of this model are as follows. (1) Water is transported from the poles to mid-latitudes during periods of high obliquity, forming a water-rich snow layer[5,6,11,12]. (2) Melting occurs at low obliquity as mid-latitude temperatures increase, producing liquid water that is stable beneath an insulating layer of overlying snow. (3) Gullies form on snow-covered slopes through erosion by melt water or as a result of melt water seeping into the loose slope materials and destabilizing them. (4) Gullies incised into the substrate are observed where the snow layer has been completely removed. (5) Patches of snow remain today where they are protected against sublimation by a layer of desiccated dust/sediment[13]. (6) Melting could be occurring at present in favourable locations in these snowpacks.

Evidence for this model is provided by unusual deposits commonly found in the mid-latitudes that may be remnants of an ice-rich mantle[2,13,14] (Figs 1 and 2). These deposits preferentially occur on cold, pole-facing slopes, can have features suggestive of flow (Fig. 2), are ~1–10 m thick, have a distinct, rounded edge marking the upslope boundary (Fig. 2), and can occur in hollows at several heights on the same knob (Fig. 1). These characteristics suggest a volatile-rich layer that was once more extensive but which has been removed from all but the cold, pole-facing slopes[2,14]. The position of the upslope boundary is significant to this model, and probably represents the highest point on the pole-facing slope where ice-rich material is stable under solar illumination.

Figure 3 illustrates the association of gullies with this volatile-rich mantling unit. Patches of smooth mantle remain on the pole-facing (north) interior wall, but gullies incised into the western crater wall are observed where the mantle has been removed. Gullies also occur in the mantle at several locations. The sequence of gully evolution is present in this crater, beginning with a shallow depression in the mantle (northwest wall), progressing to gullies incised into the mantle (north wall), and concluding with gullies incised into the substrate and the snow layer completely gone on the western wall. Figure 4 shows another example of the association of gullies with the mantling unit. Gullies are present where the overlying mantling unit has been removed, but are absent and presumably buried where the mantle remains. Significantly, the uppermost position of the mantle matches the height at which gullies begin, consistent with the mantling unit providing the source of water to carve these gullies.

Several authors have considered the conditions under which snow will accumulate and melt in non-polar regions of Mars[5,7,11,12,15–17]. Ice removed from the polar regions is transported

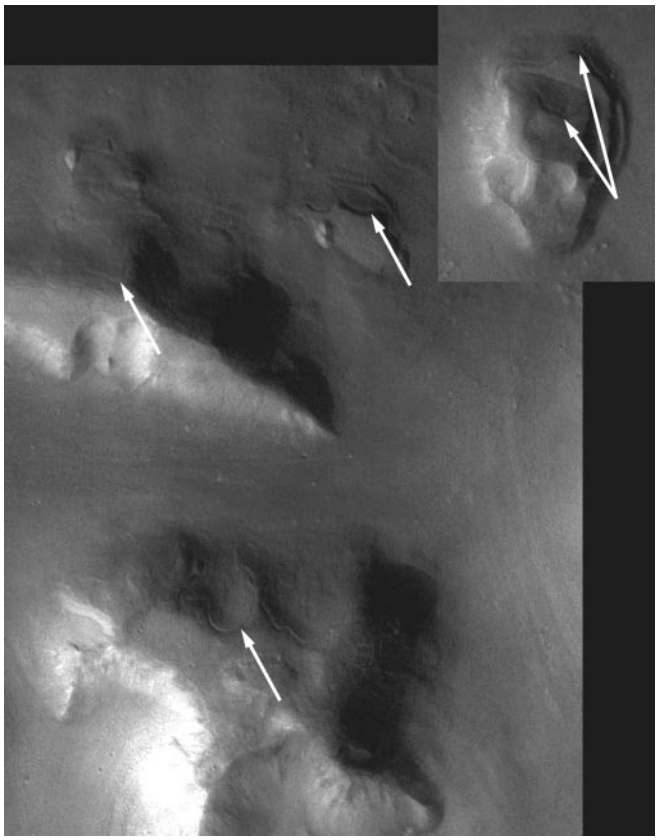

Figure 1 Examples of mid-latitude, pole-facing mantling materials and their curvilinear upper boundaries (arrows). This Mars Odyssey Thermal Emission Imaging System (THEMIS) visible-band image (V01024003) is located at approximately 40.1° N, 350.1° E, and shows the mantling terrains on pole-facing slopes at multiple elevations (arrows). The main portion of the image shown covers an area of about 8.1 × 10.6 km at 18 m per pixel. The inset shows a separate portion of the same image about 5 km to the northeast at the same scale. North is towards the top, and illumination is from the left.

equatorward at rates that are a function of obliquity[5,6,11,12], which varies from 15° to >35° on timescales of 10^5–10^6 yr (ref. 18). At maximum obliquity, a layer of ice ~0.5–2 cm in thickness could be removed from the summer cap each year and deposited at mid-latitudes[5,6]. This layer is predominately water, with minor amounts of dust incorporated as ice nucleation centres or accumulated from airfall, similar to the "dirty water ice" found in the north polar residual cap[19]. Poleward transport of water to the winter cap will also occur, but at a rate estimated to be 5–50 times slower[5,6], resulting in a net accumulation of ~0.1 cm of water ice between 30° and 50° latitude each year. Conditions favourable for water transport last several thousand years during each obliquity cycle, producing a snow layer up to ~10 m thick[5,6].

The melting of snow deposits has been modelled by Clow[7] for differing conditions of snow thickness, atmospheric pressure, snow properties, dust content, and latitude. Melting occurs beneath the surface at temperatures well below freezing, because sunlight is absorbed at depth rather than at the surface, and this absorption is substantially increased by the incorporation of minor amounts of dust[7]. Melting can occur for a wide range of snow properties and atmospheric pressures, and occurs under current conditions in mid-latitudes if dust abundances are greater than ~1,000 parts per million by mass (p.p.m.m.) (ref. 7). These dust-to-ice mixing ratios are readily attained in the present martian atmosphere, and are comparable to the polar ice deposits[19]. Meltwater moving downwards under gravity will encounter lower temperatures and refreeze. However, conduction and latent heat transfer will gradually warm the snow and substrate, allowing liquid water to accumulate and be available for erosion[7]. Subsurface erosion and collapse of the snow mantle will occur, with liquid water potentially reaching and eroding the substrate as the snow layer continues to melt. Liquid water will begin to be generated ~100 d after the spring equinox under current conditions for snow with a dust content of 1,000 p.p.m.m., and will reach a depth of 20 cm approximately 25 d later[7]. Up to 0.33 mm of snowmelt runoff is produced each day for ~50 d each martian year[7].

Typical alcove size and spacing (~200 × 200 m) provides ~4×10^4 m^2 of source snowpack for each gully, with melting of 0.25 mm per day producing ~10 m^3 of liquid water feeding each gully. For typical gully sizes of 20 m average width, 500 m length, and 10 m depth, a total of 1×10^5 m^3 of sediment has been removed from each gully. Gullies occur on steep slopes, and typically cut into what appear to be unconsolidated materials that have accumulated on these slopes. Freeze/thaw action under snow would further the breakdown of the substrate materials. Loose sediment can be transported by runoff with a water-to-sediment ratio of ~10:1 (ref. 20); transport by debris flow requires significantly less water, whereas erosion of bedrock would require more. Assuming loose debris, the total volume of gully material could be removed in 10^5 days of runoff or ~5,000 elapsed years, and gullies could readily form within the 500,000 yr since the last period of high obliquity. Multiple cycles of snow accumulation and gully erosion probably occur, reinvigorating gullies and expanding their size over several obliquity cycles. There is a strong correlation between the latitudes where ice-rich mantles and gullies occur. However, it is not expected that all snow accumulation sites will have gullies. Gullies would not form where snow accumulation is too thin, the surface too cold, or snow removal too rapid to allow melt to reach the substrate before the snow is removed. Gullies may also remain hidden beneath remnant snow. Although pole-facing, mid-latitude slopes are favoured, gullies could form anywhere that snow accumulates and melts.

Melting of snow can produce a variety of landforms. Water/ice/sediment slurries may develop and catastrophically fail, producing the levees and other features observed on some gullies that are reminiscent of debris flows[4]. Depositional fans and levees may form

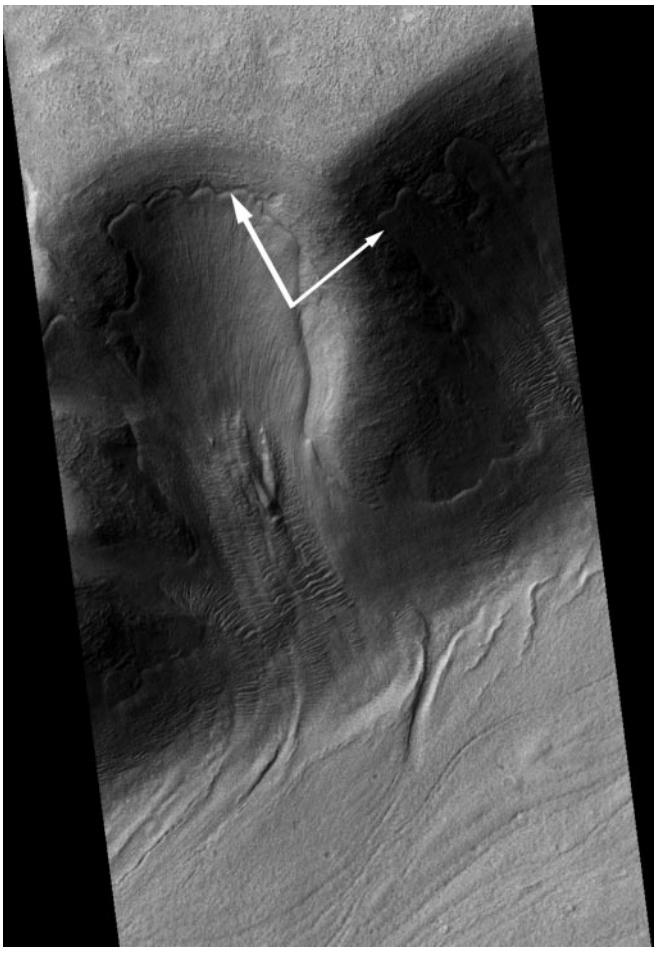

Figure 2 Detail of the appearance and curvilinear upper boundary (arrows) of pole-facing mantling materials located in Dao Valles. The surface morphology of the mantle is suggestive of flow. This Mars Global Surveyor Mars Orbiter Camera (MOC) image (M03-04950[26]) is centred at 35.7° S, 90.9° E. The portion of the image shown covers an area of about 2.8 × 5 km at 2.8 m per pixel; north is towards the top, the pole is towards the bottom, and illumination is from the left.

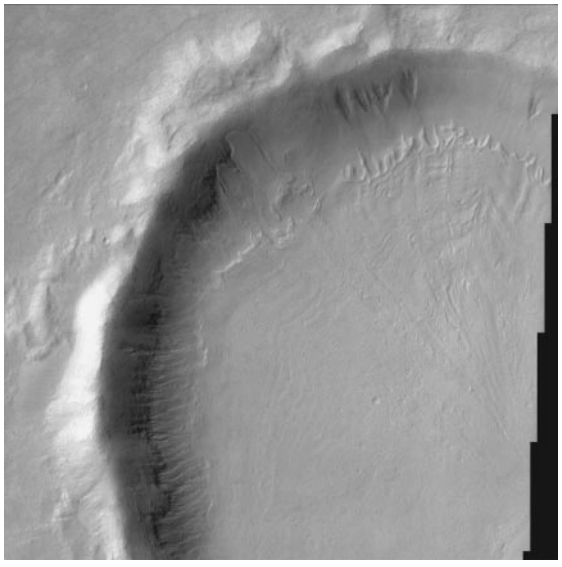

Figure 3 THEMIS image showing gullies emerging from beneath and within a mantling snow unit where this unit is being removed. This portion of a THEMIS image (V01229004; 43.0° S, 214.4° E) covers an area of about 16.2 × 16.2 km at 18 m per pixel; north is towards the top, illumination is from the left.

Figure 4 MOC image of gullies with a remnant of the snow mantle (arrow) proposed to be the source of water that eroded these gullies. This portion of image M09-2875[26] covers an area of about 2.8 × 4.5 km at 2.8 m per pixel near 33.3° S, 92.9° E; north is towards the top, illumination is from the left.

beneath the relatively thin snowpack, or slurries may travel downslope and deposit on the snow mantle or on the substrate beyond where the snow is stable. Erosion and gully formation can occur within the snow mantle itself, or overlying snow may collapse into buried gullies (Fig. 3).

Snowmelt can explain many of the unusual gully characteristics. It is not necessary to maintain or recharge a near-surface aquifer system; the source of the water comes from an overlying, atmospherically derived condensate, and the recent age reflects recent climate fluctuations capable of producing surficial water-ice deposits[5–7,11,17]. The overlying snow provides thermal insolation and a barrier against vapour diffusion, allowing liquid water to form and carve the observed gullies. The initiation of gullies within several hundred metres of crater and cliff rims[1,2] is related to the distance below the rim where snow is stable against sublimation during melting and runoff (Figs 2 and 4). Melting of a draping snow layer accounts for the development of gullies near the summit of isolated knobs where subsurface aquifers are lacking. Finally, gullies occur in clusters where water-ice accumulation and subsequent melting are optimized; water-ice is less likely to accumulate in equatorial zones[7,13], and high latitudes (>70°) may be too cold to produce melting and gully formation[7].

In the model proposed here at least some mid-latitude mantles were deposited on the surface with high ice-to-soil ratios. High (>50% volume) water-ice abundances have been found in the upper few metres at high latitudes[21–23], suggesting that this ice also formed at the surface rather than in pores. A pervasive surface texture found from 30° to 50° in both hemispheres has been interpreted to result from ice-cemented soils, 1–10 m thick, that have formed recently and are currently being devolatilized and eroded[13]. Ice is proposed to form through vapour diffusion into pore space[13,24]. However, the poleward transition from a dissected to continuous surface on this mantle corresponds to a sharp increase in near-surface ice abundance[25], suggesting that the mid-latitude portion of this mantle may be the same ice-rich material whose upper few metres have been thoroughly desiccated. In this case these terrains may have substantially more water than previously suggested[13].

The model presented here predicts that most gullied surfaces will not be sites of near-surface water reservoirs because the source snow is now gone. In addition, gully formation by snowmelt should not produce salt or mineral deposits, a prediction opposite to what might be expected if the source water was subsurface brines[9]. Finally, the near-freezing temperatures and short duration of gully formation are not likely to cause significant chemical weathering or mineralization of the surface materials.

Snowmelt has important implications for the search for life on Mars and the potential for human exploration. Liquid water is produced within several tens of centimetres of the surface, is stable for extended periods of time, and is regenerated on relatively short (10^5–10^6 yr) timescales associated with the variations in orbital parameters. Repeated access to near-surface liquid water could provide a means for life to have survived over extended periods of martian history, and could provide favourable sites for extant life today. The potential for near-surface liquid water on Mars, currently or in the recent past, within centimetres of the surface in remnant snow deposits could influence the rationale for the search for future landing and sample return sites. The rock layers above gullies, previously thought to be the water source, are extremely difficult to access and are unlikely landing sites. However, the pole-facing mantles provide an excellent opportunity to sample and study water-rich units. □

Received 4 September 2002; accepted 14 January 2003; doi:10.1038/nature01436.
Published online 19 February 2003.

1. Malin, M. C. & Edgett, K. S. Evidence for recent ground water seepage and surface runoff on Mars. *Science* **288,** 2330–2335 (2000).
2. Malin, M. C. & Edgett, K. S. Mars Global Surveyor Mars Orbiter Camera: Interplanetary cruise through primary mission. *J. Geophys. Res.* **106,** 23429–23570 (2001).
3. Mellon, M. T. & Phillips, R. J. Recent gullies on Mars and the source of liquid water. *J. Geophys. Res.* **106,** 23165–23180 (2001).
4. Costard, F., Forget, F., Mangold, N. & Peulvast, J. P. Formation of recent martian debris flows by melting of near-surface ground ice at high obliquity. *Science* **295,** 110–113 (2002).
5. Jakosky, B. M. & Carr, M. A. Possible precipitation of ice at low latitudes of Mars during periods of high obliquity. *Nature* **315,** 559–561 (1985).
6. Jakosky, B. M., Henderson, B. G. & Mellon, M. T. Chaotic obliquity and the nature of the Martian climate. *J. Geophys. Res.* **100,** 1579–1584 (1995).
7. Clow, G. D. Generation of liquid water on Mars through the melting of a dusty snowpack. *Icarus* **72,** 95–127 (1987).
8. Knauth, L. P., Klonowski, S. & Burt, D. Ideas about the surface runoff features on Mars. *Science* **290,** 711–712 (2000).
9. Knauth, L. P., Burt, D. M. & Tyburczy, J. A. in *Conference on the Geophysical Detection of Subsurface Water on Mars* 60–61 (Lunar and Planetary Institute Contribution No. 1095, Houston, Texas, 2001).
10. Musselwhite, D. S., Swindle, T. D. & Lunine, J. I. Liquid CO_2 breakout and the formation of recent small channels on Mars. *Geophys. Res. Lett.* **28,** 1283–1285 (2001).
11. Toon, O. B., Pollack, J. B., Ward, W., Burns, J. A. & Bilski, K. The astronomical theory of climate change on Mars. *Icarus* **44,** 552–607 (1980).
12. Haberle, R. M. *et al.* On the possibility of liquid water on present-day Mars. *J. Geophys. Res.* **106,** 23317–23326 (2001).
13. Mustard, J. F., Cooper, C. D. & Rifkin, M. K. Evidence for recent climate change on Mars from the identification of youthful near-surface ground ice. *Nature* **412,** 411–414 (2001).
14. Carr, M. H. Mars Global Surveyor observations of fretted terrain. *J. Geophys. Res.* **106,** 23571–23595 (2001).
15. Gulick, V. C., Tyler, D., McKay, C. P. & Haberle, R. M. Episodic ocean-induced CO_2 greenhouse on Mars: Implications for fluvial valley formation. *Icarus* **130,** 68–86 (1997).
16. Lee, P., Cockell, C. S., Marinova, M. M., McKay, C. P. & Rice, J. W. Snow and ice melt flow features in Devon Island, Nunavut, Arctic Canada as possible analogs for recent slope flow features on Mars. (abstract) *Lunar Planet. Sci.* [CD-ROM] 1809 (2001).
17. Hecht, M. H. Metastability of liquid water on mars. *Icarus* **156,** 373–386 (2002).
18. Ward, W. R. Present obliquity oscillations of Mars: Fourth-order accuracy in orbital E and I. *J. Geophys. Res.* **84,** 237–241 (1979).
19. Kieffer, H. H., Chase, S. C. Jr, Martin, T. Z., Miner, E. D. & Palluconi, F. D. Martian North Pole summer temperatures: Dirty water ice. *Science* **194,** 1341–1344 (1976).
20. Howard, A. D. & C.F. McLane, I. Erosion of cohesionless sediment by groundwater seepage. *Water Resour. Res.* **24,** 1659–1674 (1988).
21. Feldman, W. C. *et al.* Global distribution of neutrons from Mars: Results from Mars Odyssey. *Science* **297,** 75–78 (2002).
22. Mitrofanov, I. *et al.* Maps of subsurface hydrogen from the high energy neutron detector, Mars Odyssey. *Science* **297,** 78–81 (2002).
23. Boynton, W. V. *et al.* Distribution of hydrogen in the near surface of Mars: Evidence for subsurface ice deposits. *Science* **297,** 81–85 (2002).
24. Mellon, M. T. & Jakosky, B. M. The distribution and behavior of martian ground ice during past and present epochs. *J. Geophys. Res.* **100,** 11781–11799 (1995).

25. Tokar, R. L. *et al.* Ice concentration and distribution near the South Pole of Mars: Synthesis of Odyssey and Global Surveyor analyses. *J. Geophys. Res.* **29,** doi:1029/2002GL015691 (2002).
26. Malin, M. C. *et al.* Image M17-00423, Malin Space Science Systems Mars Orbiter Camera Image Gallery at ⟨http://www.msss.com/moc_gallery⟩ (2002).

Acknowledgements I thank the THEMIS instrument development team at Arizona State University and Raytheon Santa Barbara Remote Sensing, and the spacecraft development and operations teams at the Jet Propulsion Laboratory and Lockheed Martin Astronautics, for the development and performance of the THEMIS instrument and the Odyssey spacecraft. I also thank J. Rice, S. Ruff, H. Kieffer, M. Malin and B. Jakosky for discussions and contributions, and M. Carr and J. Mustard for comments that improved the original manuscript. This work was supported through the NASA Mars Odyssey Project and the NASA Mars Data Analysis Program.

Competing interests statement The author declares that he has no competing financial interests.

Correspondence and requests for materials should be addressed to the author (e-mail: phil.christensen@asu.edu).

Three-dimensional imaging of atomic four-body processes

M. Schulz*†, R. Moshammer*, D. Fischer*, H. Kollmus*, D. H. Madison†, S. Jones† & J. Ullrich*

** Max-Planck Institut für Kernphysik, Saupfercheckweg 1, D 69117 Heidelberg, Germany*
† University of Missouri-Rolla, Physics Department and Laboratory for Atomic, Molecular, and Optical Research, Rolla, Missouri 65409, USA

To understand the physical processes that occur in nature we need to obtain a solid concept about the 'fundamental' forces acting between pairs of elementary particles. It is also necessary to describe the temporal and spatial evolution of many mutually interacting particles under the influence of these forces. This latter step, known as the few-body problem, remains an important unsolved problem in physics. Experiments involving atomic collisions represent a useful testing ground for studying the few-body problem. For the single ionization of a helium atom by charged particle impact, kinematically complete experiments have been performed[1–6] since 1969 (ref. 7). The theoretical analysis of such experiments was thought to yield a complete picture of the basic features of the collision process, at least for large collision energies[8–14]. These conclusions are, however, almost exclusively based on studies of restricted electron-emission geometries[1–3]. Here, we report three-dimensional images of the complete electron emission pattern for the single ionization of helium by the impact of C^{6+} ions of energy 100 MeV per a.m.u. (a four-body system) and observe features that have not been predicted by any published theoretical model. We propose a higher-order ionization mechanism, involving the interaction between the projectile and the target nucleus, to explain these features.

The experimental set-up[15] is shown schematically in Fig. 1. C^{6+} projectiles of 100 MeV per a.m.u. collided with cold (<1K) He gas target atoms from a supersonic jet. The recoiling target ions and the ionized electrons were extracted by a weak electric field and detected by two-dimensional position-sensitive channel plate detectors. A uniform magnetic field of 12 G ($1\,G = 10^{-4}\,T$) parallel to the electric field forced the electrons into cyclotron motion (green spiral line). It thereby confined their motion in the plane perpendicular to the extraction field (transverse plane), so that all electrons with a transverse momentum of less than 2 atomic units (a.u.) hit the detector. Both particles were measured in coincidence with the projectiles, which did not change charge state. The momentum components of the recoil ion and the electron in the direction of the extraction field (longitudinal components) were determined from the time of flight of each particle from the collision region to the respective detector. The transverse momenta were obtained from the position information provided by the detectors for a fixed time of flight.

In Fig. 2a the measured three-dimensional fully differential cross-sections (FDCS) are shown as a function of the azimuthal (φ_e) and polar (θ_e) electron angles. Although the data are only shown for a momentum transfer (defined as the difference between the initial and scattered projectile momentum) of q = 0.75 a.u. and an ionized electron energy $E_e = 6.5$ eV, all other final electron energies $E_e < 50$ eV and a large fraction of all possible momentum transfers are recorded simultaneously but not discussed in this letter. The initial projectile direction is along the z axis and **q** is pointing nearly in the x direction. φ_e is measured in the x–y plane relative to the x axis, that is $\varphi_e = 0°$ and 180° correspond to the scattering plane (the plane spanned by the initial projectile momentum and the momentum transfer vectors). θ_e is the angle of the electron momentum vector relative to the z axis.

The characteristic double-lobe structure with peaks at ($\theta_e = 90°$, $\varphi_e = 0°$) and ($\theta_e = 90°$, $\varphi_e = 180°$) well-known from high-energy electron-impact studies in the scattering plane[1–3] is clearly observable. The ($\theta_e = 90°$, $\varphi_e = 0°$) maximum (called the binary peak), which occurs in the direction of **q**, is relatively easy to understand. It is due to collisions which are dominated by a binary interaction between the projectile and the electron, that is, the recoil ion remains essentially passive. Momentum conservation then demands that the electron be emitted approximately in the direction of **q**. The ($\theta_e = 90°$, $\varphi_e = 180°$) lobe (called the recoil peak), has been interpreted as a double scattering process[16]: the electron, initially emitted approximately in the direction of **q**, on its path out of the atom elastically backscatters from the recoil ion, which picks up most of the momentum transferred from the projectile.

We expect the ionization cross-sections at the small perturbations Z_p/v_p (where Z_p and v_p are the atomic number and the velocity of the projectile) studied in this work to be essentially identical for electron and ion impact. Furthermore, the results of various theoretical approaches converge with each other with decreasing perturbation. For our collision system, it is therefore not critical which model is used for comparison with the data in order to identify potential deviations from our current understanding. We chose a continuum distorted wave approach with Hartree–Fock wavefunctions for the active electron (CDW–HF), because it is the most powerful model currently available for ion impact ionization.

Figure 2b shows our theoretical FDCS for the same conditions as the experimental data. This CDW–HF calculation is based on refs 10

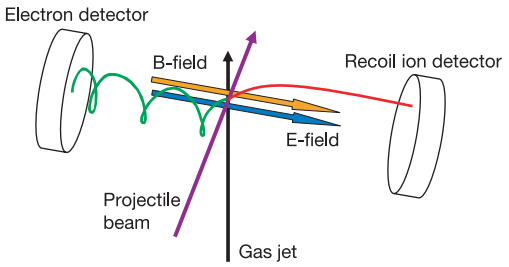

Figure 1 Schematic experimental set-up for three-dimensional imaging of atomic processes. The projectile-ion beam (purple arrow) is crossed with an atomic He beam from a supersonic gas jet (black arrow). The ionized electrons and the recoiling target ions are extracted by a weak electric field (blue arrow) and detected by two-dimensional position-sensitive detectors. A pair of Helmholtz coils generates a uniform magnetic field (B-field, yellow arrow) which forces the electrons into cyclotron trajectories (green spiral line) and guides them onto the detector. Two electronic clocks are used to measure the time of flight of the electrons and the recoil ions from the collision region to the respective detector.

